Broadband Rational Macromodeling Based on the Adaptive Frequency Sampling Algorithm and the Partial Element Equivalent Circuit Method

Giulio Antonini, *Senior Member, IEEE*, Dirk Deschrijver, and Tom Dhaene, *Senior Member, IEEE*

Abstract—The increasing operating frequencies in modern designs call for broadband macromodeling techniques. The problem of computing high-accuracy simulation models for high-speed interconnects is of great importance in the modeling arena. Nowadays, many full-wave numerical techniques are available that provide high accuracy, often at a significant cost in terms of memory storage and computing time. Furthermore, designers are usually only interested in a few electrical quantities such as port voltages and currents. So, model order reduction techniques are commonly used to achieve accurate results in a reasonable time. This paper presents a new technique, based on the partial element equivalent circuit method, which allows to generate reduced-order models by adaptively selecting the complexity (order) of the macromodel and suitable frequency samples. Thus, the proposed algorithm allows to limit the computing time while preserving the accuracy. Validation examples are given.

Index Terms—Adaptive frequency sampling (AFS), electromagnetic transient analysis, fitting techniques, frequency response, partial element equivalent circuit (PEEC) method.

I. INTRODUCTION

NOWADAYS, full-wave electromagnetic (EM) methods [1]–[3] are widely used to simulate a variety of complex high-speed systems and are considered to be essential for efficient design. The use of these methods usually results in the computation of a huge number of field (E, H) or circuit (i, v) unknowns, in the frequency domain (FD) or time domain (TD), although users are usually only interested in a few of them at the input and output ports. The reduction of the complexity of the linear simulation model, as defined by the full-wave numerical method, is crucial to reduce the overall computational cost required to characterize the system over a desired frequency range. So, the development of a compact macromodel of the EM system has become a topic of intense research over the last years. Important applications of EM-based modeling include high-speed packages, interconnects, vias, and on-chip passive components [4]–[8].

G. Antonini is with the UAq Electromagnetic Compatibility Laboratory, Dipartimento di Ingegneria Elettrica e dell'Informazione, Università degli Studi di L'Aquila, L'Aquila 67040, Italy (e-mail: antonini@ing.univaq.it).

D. Deschrijver and T. Dhaene are with the Department of Information Technology (INTEC), Ghent University, Ghent 9000, Belgium (e-mail: dirk.deschrijver@intec.ugent.be; tom.dhaene@intec.ugent.be).

Over the years, several techniques have been developed to speed up the EM analysis of such complex systems. They can be classified in two groups: 1) acceleration techniques and 2) model order reduction (MOR) techniques.

The first group aims to accelerate the solution of the huge linear systems yielded by the discretization of Maxwell's equations. This class includes fast techniques such as the fast multipole method (FMM) [9]–[11], the multilevel fast multipole method (MLFMM) [12]–[14], the precorrected fast Fourier transform accelerated method of moments (MoMs) [15], [16], and the QR decomposition [17], [18].

The MOR techniques aim to reduce the overall system complexity while retaining the important features of the original system. Two major MOR techniques can be distinguished: model-driven MOR and data-driven MOR. In model-driven MOR, the full set of model equations are available for reduction, while in data-driven MOR, only the data at the inputs and outputs are available to build reduced macromodels. Model-driven MOR for circuit applications was first introduced in [19]–[21]. Since then, many researchers have developed the MOR techniques and applied to electrical circuits [22]–[26]. More recently, a passive reduced-order interconnect macromodeling algorithm, known as PRIMA [27], has received great attention due to its capability to generate passive macromodels of resistive–inductive–capacitive (RLC) circuits, which is important because stable, but nonpassive, macromodels can produce unstable systems when connected to other stable, even passive, loads.

The integral-equation-based methods describe near- and far-field interactions by means of a proper Green's function where the time delay appears in the integrals describing the electric and magnetic field couplings. Among the integral-equation-based methods, the partial element equivalent circuit (PEEC) method has gained an increasing popularity among electromagnetic compatibility (EMC) engineers due to its capability to provide a circuit interpretation of the electric field integral equation (EFIE), thus allowing to handle complex problems involving EM fields and circuits [7], [28], [29].

In [30], an MOR of PEEC circuits including delays is presented. To obtain an MOR for systems with delays, a Padé approximation of the exponential term $e^{-s\tau}$ is adopted. Then, the relevant region Ω in the s-complex plane is subdivided into smaller regions Ω_i, for $1 \le i \le I$, and an iterative method is used to obtain an approximation for the transfer function of the linear system in each subregion; all portions of the transfer functions are finally combined to obtain an approximation of the original PEEC system.

Over the last 20 years, data-driven MOR techniques have received great interest, based on the the pioneering works of

Miller [31]–[34]: when the system is characterized at a discrete set of frequencies, rational least-squares approximation techniques can be used to generate accurate reduced FD macromodels of complex EM systems. However, it is known that they often suffer from poor numerical conditioning in the case of broadband characterization.

Gustavsen and Semlyen [35] recently proposed an iterative macromodeling technique, called vector fitting (VF) that uses partial fraction basis functions to approximate the frequency samples. A set of initial poles is relocated in successive iterations until convergence is obtained. The technique is robust, due to the use of rational basis functions instead of polynomials, and has been widely used in different areas ranging from power systems [36] to high-speed interconnects [37], EMC [38], and signal integrity (SI) [39] problems.

Data-based MOR techniques are driven by a set of FD data samples, which are selected over a specified frequency range of interest. These samples can be obtained from measurements or numerical simulations, which are usually time-consuming. When using numerical solvers, both the TD and FD analysis techniques can be adopted to generate the frequency response data. The TD techniques are usually faster than their FD counterpart, but, as explained earlier, frequency-dependent phenomena (e.g., skin effect, dielectric losses) require a significant additional effort to be modeled; on the other hand, FD techniques can manage very easily frequency-dependent phenomena but at a larger computational solution cost as matrices describing the couplings need to be reevaluated at each frequency sample. A combination of oversampling and straight-line interpolation is often used to represent the frequency behavior over a frequency range of interest, but it implies a waste of time and computer resources. If the sampling rate is reduced, undersampling may occur that may result in a loss of important features of the response. Even if most of the desired frequency range is oversampled, some important features can still be missed due to local undersampling. Usually, some prior knowledge of the dynamics of the EM system is required in order to select an appropriate sample distribution and an appropriate model complexity to accurately model the spectral response of a system [31], [40].

This paper presents an adaptive sample selection and modeling scheme used in combination with the PEEC [2] to generate rational macromodels of EM systems at a reduced computational cost. The *adaptive frequency sampling* (AFS) algorithm [41] selects a limited number of frequency data samples in consecutive iterations and interpolates the data using rational fitting models. The adaptive algorithm does not require any prior knowledge of the system to select a suitable sample distribution and the model complexity. It allows important details to be modeled by automatically sampling the response of the system more densely at the corresponding frequencies. The PEEC method is used as a full-wave EM tool to generate the required frequency samples.

We start in Section II with a brief description of the PEEC method that provide a circuit interpretation of the EFIE, thus allowing to study the EM problem in terms of Kirchhoff's laws. Next, in Section III, we present the AFS algorithm that generates the rational macromodel of the system by adaptively selecting frequency samples and the order of the model. Sections IV and V present computational results and conclusions, respectively.

II. PEEC FORMULATION

The classical PEEC method [28] is derived from the equation for the total electric field that holds at any point in a conductor; in the complex domain, it reads

$$\boldsymbol{E}^i(\boldsymbol{r}, s) = \frac{\boldsymbol{J}(\boldsymbol{r}, s)}{\sigma} + \frac{s\mu}{4\pi} \int_{V'} \frac{\boldsymbol{J}(\boldsymbol{r}', s) \, e^{-s\tau}}{|\boldsymbol{r} - \boldsymbol{r}'|} \, dV'$$
$$+ \nabla \frac{1}{4\pi\varepsilon} \int_{S'} \frac{\varrho(\boldsymbol{r}', s) e^{-s\tau}}{|\boldsymbol{r} - \boldsymbol{r}'|} \, dS' \quad (1)$$

where $\boldsymbol{E}^i(\boldsymbol{r}, s)$ is the incident electric field at the observation point $\boldsymbol{r}$, $\boldsymbol{J}(\boldsymbol{r}, s)$ and $\varrho(\boldsymbol{r}', s)$ are the current and charge densities at the source point $\boldsymbol{r}'$, $\tau = |\boldsymbol{r} - \boldsymbol{r}'|/c_0$, c_0 is the speed of light in the free space, and s is the Laplace variable.

The most popular method for the discretization of integral equations was called the MoMs by Harrington [1] and has different implementations [42]–[45]. In PEEC, the unknown quantities $\boldsymbol{J}(\boldsymbol{r}, s)$ and $\varrho(\boldsymbol{r}, s)$ are expanded as a weighted sum of a finite set of basis functions, in the first step. Next, the Galerkin's testing or weighting process [46] is used to generate a system of equations for the unknowns weights. Unlike the MoMs, the PEEC method discretizes volumes for modeling current density and surfaces for charge density. The discretization process generates topological elements, branches, and nodes and, as a consequence, an equivalent circuit. The enforcement of the discrete form of (1) to each branch and the continuity equation to each node is equivalent to enforce Kirchhoff voltage law (KVL) and Kirchhoff current law (KCL) to the equivalent circuit.

Enforcing Kirchhoff's voltage and current laws to N_I independent loops and N_ϕ independent nodes of the PEEC equivalent circuit yields

$$-\boldsymbol{A}\boldsymbol{\Phi}(s) - \boldsymbol{R}\boldsymbol{I}_L(s) - s\boldsymbol{L}_p(s)\boldsymbol{I}_L(s) = \boldsymbol{V}_s(s) \quad (2a)$$
$$s\boldsymbol{P}^{-1}(s)\boldsymbol{\Phi}(s) - \boldsymbol{A}^t\boldsymbol{I}_L(s) = \boldsymbol{I}_s(s) \quad (2b)$$

where
1) $\boldsymbol{\Phi}(s) \in \Re^{N_\phi}$ is the vector of node potentials to infinity; $\Re^{N_\phi}$ is the node space of the equivalent network;
2) $\boldsymbol{I}_L(s) \in \Re^{N_I}$ is the vector of currents including both conduction and displacement currents; $\Re^{N_I}$ is the current space of the equivalent network;
3) $\boldsymbol{L}_p(s)$ is the matrix of partial inductances describing the magnetic field coupling;
4) $\boldsymbol{P}(s)$ is the matrix of coefficients of potential describing the electric field coupling, $\boldsymbol{\Phi}(s) = \boldsymbol{P}(s)\boldsymbol{Q}(s)$, where $\boldsymbol{Q}(s)$ is the charge on each panel of the conductor surface;
5) $\boldsymbol{R}$ is the matrix of resistances;
6) $\boldsymbol{A}$ is the connectivity matrix;
7) $\boldsymbol{V}_s(s)$ is the vector of distributed voltage sources due to external EM fields [47];
8) $\boldsymbol{I}_s(s)$ is the vector of lumped current sources.

The partial elements, namely partial inductances $\boldsymbol{L}_p(s)$ and coefficients of potential $\boldsymbol{P}(s)$, are frequency-dependent as a consequence of nature of the Green's function for the free space $G(\boldsymbol{r} - \boldsymbol{r}', s) = e^{-s\tau}/|\boldsymbol{r} - \boldsymbol{r}'|$.

In order to avoid any matrix inversion, (2b) can be rewritten as

$$s\boldsymbol{\Phi}(s) - \boldsymbol{P}(s)\boldsymbol{A}^t\boldsymbol{I}_L(s) = \boldsymbol{P}(s)\boldsymbol{I}_s(s). \quad (3)$$

The EMC and SI engineers are usually only interested in a few electrical quantities, such as port and current voltages. For TD simulations, compact rational macromodels are strongly desired. In this perspective, the AFS algorithm [41] is used, in conjunction with an PEEC frequency solver, to build a rational macromodel of the PEEC equivalent circuit.

III. ADAPTIVE SAMPLING ALGORITHM

Full-wave techniques (such as the FDTD or PEEC method) are very accurate; however, they can often be time-consuming and resource demanding. The computation time to calculate frequency samples might take so long that one limits the number of data in order to get results in a moderate amount of time. If the sampling rate is reduced, undersampling may occur, which means that some important features, such as coupling effects and resonances, can be missed. Even if most of the desired frequency range is oversampled, some important effects can still be missed due to local undersampling. Traditionally, some *a priori* knowledge of the system dynamics is required in order to select an appropriate sample distribution and an appropriate model complexity to represent the impedance matrix of the structure in an accurate way. In this paper, an efficient rational modeling scheme is applied to overcome this problem by combining the use of VF and AFS.

A. Vector Fitting

The rational macromodel $R_{mn}(j\omega)$ (for $m, n = 1, \ldots, N$) of an N-port system is represented as a partial fraction expansion

$$R_{mn}(j\omega) = \sum_{p=1}^{P} \frac{c_{mn,p}}{j\omega - a_p} + d_{mn} \approx Z_{mn}(j\omega) \qquad (4)$$

provided that $\boldsymbol{c} = \{c_{mn,p}\}_{p=1}^{P}$ is a vector that contains the residues, corresponding to the matrix element Z_{mn}, and d_{mn} represents the associated element of the feedthrough matrix. Each matrix element shares a common set of transfer function poles, which are denoted by a vector $\boldsymbol{a} = \{a_p\}_{p=1}^{P}$. To identify these parameters of the rational model, the VF technique can be applied. The VF is a robust macromodeling tool for rational approximation of FD responses [35]. The technique iteratively calculates a suitable set of poles, and solves the residues of the transfer function in a two-step procedure. The goal of this algorithm is to select the coefficients in such way that the least-squares distance between the model $R_{mn}(j\omega)$ and the data $Z_{mn}(j\omega)$ is minimized over all the selected frequency samples. Based on the partial fraction representation of each matrix element, the state-space realization $(\boldsymbol{A}, \boldsymbol{B}, \boldsymbol{C}, \boldsymbol{D})$ of the overall transfer function

$$\boldsymbol{R}(j\omega) = \boldsymbol{C}(j\omega\boldsymbol{I} - \boldsymbol{A})^{-1}\boldsymbol{B} + \boldsymbol{D} \qquad (5)$$

is directly obtained as shown in [48]. An application of the inverse Laplace transformation on the state equation and the output equation yields the TD macromodel of the overall PEEC circuit, which can be written as

$$\dot{\boldsymbol{x}}(t) = \boldsymbol{A}\boldsymbol{x}(t) + \boldsymbol{B}v(t)$$
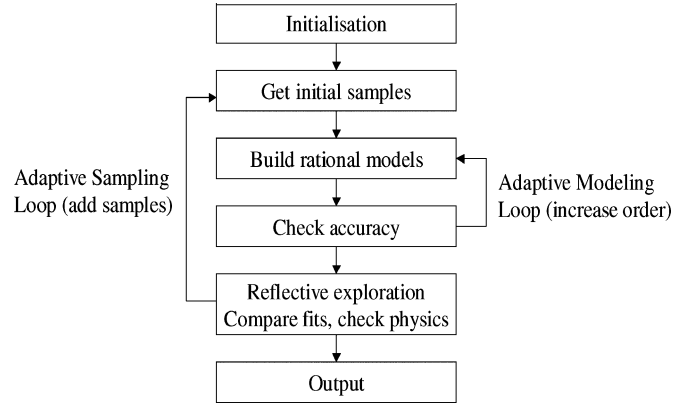$$\boldsymbol{i}(t) = \boldsymbol{C}\boldsymbol{x}(t) + \boldsymbol{D}v(t). \qquad (6)$$

Fig. 1. Flowchart of the AFS algorithm.

A standard minimal-order realization can efficiently be adopted [49]–[52]. In addition, linear and nonlinear terminations can easily be added and handled by the modified nodal analysis (MNA) [53]. The state-space realization (6) can be easily linked to standard nonlinear solvers or general purpose circuit simulators. For those circuit simulators, such as HSPICE [54], which do not directly accept a state-space representation, an equivalent circuit has to be generated. This task can be accomplished by using well-known synthesis techniques [39], [55]–[57].

B. Adaptive Modeling and Sampling Algorithm

In this section, an adaptive technique is described that automatically selects a reduced amount of data samples $[j\omega, Z_{mn}(j\omega)]$ in consecutive iterations, and approximates them by a rational macromodel [58], [59]. At the same time, the order of the rational model is kept minimal in each iteration step [41], [60]. The convergence of the algorithm is based on error estimates, which provide information about the quality of the rational model. The algorithm allows important details to be modelled by adaptively sampling the response of the structure more densely where the data are changing more rapidly. The goal is to minimize the total number of data samples needed, while maximizing the information provided by each new sample. To ensure stability of the TD simulations, passivity of the macromodel can be enforced as a postprocessing step [61]. The algorithm of the AFS is described later. It consists of an adaptive modeling loop and an adaptive sampling loop. A flowchart is shown in Fig. 1.

1) Adaptive Modeling Loop: The algorithm starts with a set (S) of four data samples that are equidistantly spread over the frequency range of interest $[\omega_{\min}, \omega_{\max}]$. Depending on the number of available data points, multiple rational fitting models $R_{mn}(j\omega)$ with different order of numerator and denominator are built for each matrix element $Z_{mn}(j\omega)$, exploiting all degrees of freedom. If the RMS error between the two best calculated fitting models and the selected data points exceeds a certain threshold δ, then the models are rejected, and the model complexity is increased iteratively.

2) Adaptive Sampling Loop: Once the selected data samples are approximated sufficiently well, the two most accurate fitting models [here denoted by $R_{mn}^1(j\omega)$ and $R_{mn}^2(j\omega)$] are selected and compared by means of a set of heuristical rules H_i, like

those shown in (7)–(13). Such rules, called reflective functions (RFs), provide an error estimate that can be used to validate the quality of the overall model. Depending on the desired accuracy of the model, the thresholds of such rules (δ_i) can be adjusted toward the user's requirement. For the examples presented in this paper, a model is considered to be sufficiently accurate, if the overall RMS error is approximately of the order 10^{-4} or better

$$H_0 : \max_{m,n} \frac{\left| R_{mn}^{(1)}(j\omega_k) - R_{mn}^{(2)}(j\omega_k) \right|}{\left| R_{mn}^{(1)}(j\omega_k) \right|} \leq \delta_0 \qquad \forall k \qquad (7)$$

$$H_1 : \max_{m,n} \frac{\left| |R_{mn}^{(1)}(j\omega_k)| - |R_{mn}^{(2)}(j\omega_k)| \right|}{\left| R_{mn}^{(1)}(j\omega_k) \right|} \leq \delta_1 \qquad \forall k \quad (8)$$

$$H_2 : \max_{m,n} \angle\left(R_{mn}^{(1)}(j\omega_k) \right) - \angle\left(R_{mn}^{(2)}(j\omega_k) \right) \leq \delta_2 \quad \forall k \quad (9)$$

$$H_3 : \max_{m,n} \sqrt{\frac{1}{K} \sum_{k=1}^{K} \left| R_{mn}^{(1)}(j\omega_k) - R_{mn}^{(2)}(j\omega_k) \right|^2} \leq \delta_3 \quad (10)$$

$$H_4 : \begin{vmatrix} u_{mn,1}^{(1)}(k, k-1) & u_{mn,2}^{(1)}(k, k-1) \\ u_{mn,1}^{(1)}(k, k+1) & u_{mn,2}^{(1)}(k, k+1) \end{vmatrix} \geqslant 0 \quad \forall k \quad (11)$$

$$\text{if} \quad \cos^{-1} \frac{\boldsymbol{u}_{mn}^{(1)}(k-1, k)^T \boldsymbol{u}_{mn}^{(1)}(k, k+1)}{\left\| \boldsymbol{u}_{mn}^{(1)}(k-1, k) \right\| \left\| \boldsymbol{u}_{mn}^{(1)}(k, k+1) \right\|} \geqslant \delta_4 \quad (12)$$

$$H_5 : \text{eig}(\text{Re}(R^{(1)}(j\omega_k))) \geqslant 0 \gg \delta_5, \qquad \forall k \qquad (13)$$

provided that

$$\boldsymbol{u}_{mn}^{(1)}(k_1, k_2) = \left[u_{mn,1}^{(1)}(k_1, k_2), u_{mn,2}^{(1)}(k_1, k_2) \right]^T \qquad (14)$$

$$u_{mn,1}^{(1)}(k_1, k_2) = \text{Re}\left(R_{mn}^{(1)}(j\omega_{k_2}) \right) - \text{Re}\left(R_{mn}^{(1)}(j\omega_{k_1}) \right) \quad (15)$$

$$u_{mn,2}^{(1)}(k_1, k_2) = \text{Im}\left(R_{mn}^{(1)}(j\omega_{k_2}) \right) - \text{Im}\left(R_{mn}^{(1)}(j\omega_{k_1}) \right). \quad (16)$$

If the estimated error of the models is too high, due to an unresolved frequency response, then the adaptive sampling loop selects additional data samples at well-chosen locations in the frequency range. The location of new frequency samples is determined by minimizing the maximum relative fitting errors of the best models with respect to the frequency. This process, called reflective exploration [62], is iteratively repeated until the largest mismatch of the response is within a predefined tolerance level, and each rule H_i is satisfied. If the impedance matrix contains multiple elements, then an optimal data sample are selected for the least converged matrix element.

C. Rational Model Validation

In a final step, two additional data samples can be computed to validate the model. The location of these data samples can be chosen where the estimated fitting error is maximal (error-based sampling), or where the distance between successive data samples is maximal (density-based sampling). It is noted that these validation samples are typically not used to build the fitting model, unless they indicate premature convergence of the algorithm. As a postprocessing step, the order can sometimes be

further reduced by resampling the AFS model sufficiently dense, and refitting the data using the relaxed vector fitting (RVF) technique [63]. It was shown that the RVF has better convergence properties than the VF approach, and, can therefore, lead to a sufficient accuracy for models with lower complexity. The resampling of the AFS model does not introduce a significant cost, since it is much cheaper to evaluate when compared to the calculation of additional frequency samples.

Input: Generator of data $Z_{ij}(j\omega)$, Frequency range $[f_{min}, f_{max}]$
Output: State-space model $SER = (A, B, C, D)$
Calculate 4 equidistant data samples $S = \{Z(s_{min}), ..., Z(s_{max})\}$

```
convergence = false;
while convergence = false do

    %Adaptive Modeling Loop
    order_found = false;
    while order_found = false do
        foreach number of poles n_min < n_p < n_max do
            foreach number of zeros n_{p-1} ≤ n_z ≤ n_{p+1} do
                | [SER_i, rmserr_i] = vectfit(S, n_p, n_z);
            end
        end
        [SER_1, rmserr_1] = select_best(SER_i, rmserr_i);
        [SER_2, rmserr_2] = select_2nd_best(SER_i, rmserr_i);
        if rmserr_1 > δ or rmserr_2 > δ then
            | n_min = n_min + 1, n_max = n_max + 1;
        else
            | order_found = true;
        end
    end

    [resp_1] = freqresp(SER_1, [f_min, f_max]);
    [resp_2] = freqresp(SER_2, [f_min, f_max]);

    %Adaptive Sampling Loop
    heuristics_ok = true;
    foreach heuristical rule H_i do
        while heuristics_ok = true do
            | heuristics_ok = heuristics_i(resp_1, resp_2);
        end
    end
    if heuristics_ok = true then
        | convergence = true;
    else
        | s_new = getfreq(max_s (|resp_1 - resp_2|/|resp_1|));
        | Z(s_new) = calculate_data(s_new);
        | S = S ∪ Z(s_new)
    end

end

SER = reduce_order(SER_1);
SER = make_passive(SER);
```

IV. NUMERICAL EXAMPLES

In this section, we demonstrate the practical value and robustness of the AFS-based PEEC solver. All the simulations have been performed on a desktop computer with an Advanced Micro Devices (AMD) processor with a 2-GHz clock frequency, 1.5 GB of RAM, and operating under Windows XP.

A. Two-Conductor Transmission Line

A two-conductor transmission line is shown in Fig. 2; the two conductors are 10 cm long and 1 cm apart. It has been modeled by the PEEC using 240 volume (inductive) cells and 336 surface (capacitive) cells, resulting in 240 currents $\boldsymbol{i}_L$ and 88 potentials $\boldsymbol{v}$ to infinity. The transmission line is terminated on two 50-Ω resistances. Fig. 3. shows the scattering parameters up to 4 GHz.
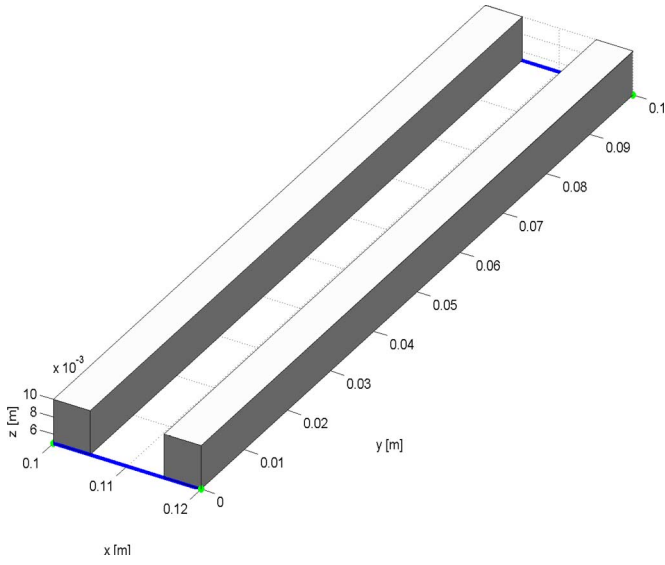
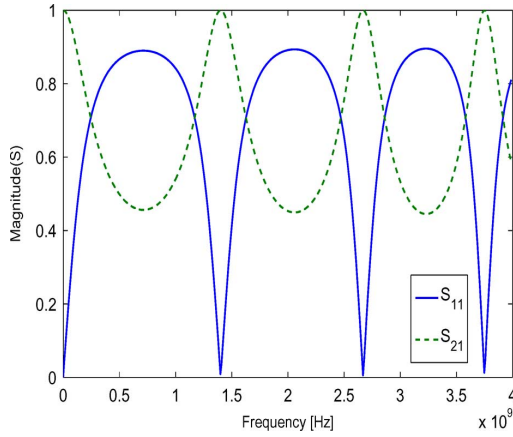Fig. 2.   Two-conductor transmission line.

Fig. 3.   Scattering parameters.

TABLE I
RMS ERROR (SETION IV-A)

Frequency samples	RMS error
4	0.207282
6	0.148747
8	0.235644
11	0.255576
14	0.086110
17	0.000397

Fig. 4.   Magnitude spectra of Y_{11} and Y_{12} admittances, using AFS modeling.
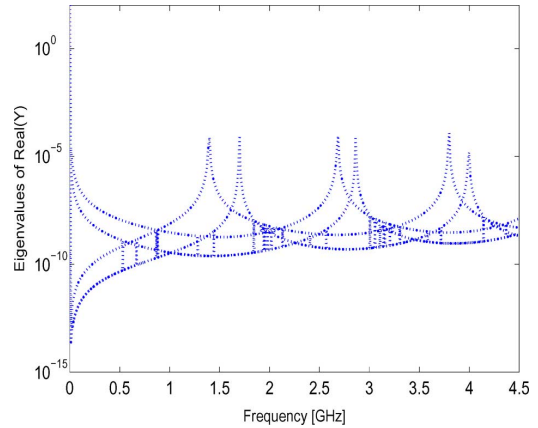
Fig. 5.   Passivity check: eigenvalues of $\mathrm{Re}(\boldsymbol{Y}(j\omega))$.

The proposed approach has been applied to generate a rational model of the $\boldsymbol{Y}$-matrix. Fig. 4 shows a comparison of the input data with the rational macromodel generated by using the AFS and shows the data samples used. In this example, 17 samples have been chosen to obtain a guaranteed macromodel accuracy of -60 dB.

As new resonances are discovered, additional frequency samples are added. Table I shows the RMS error as the AFS algorithm proceeds, rapidly reducing the fitting error by using only a limited number of samples.

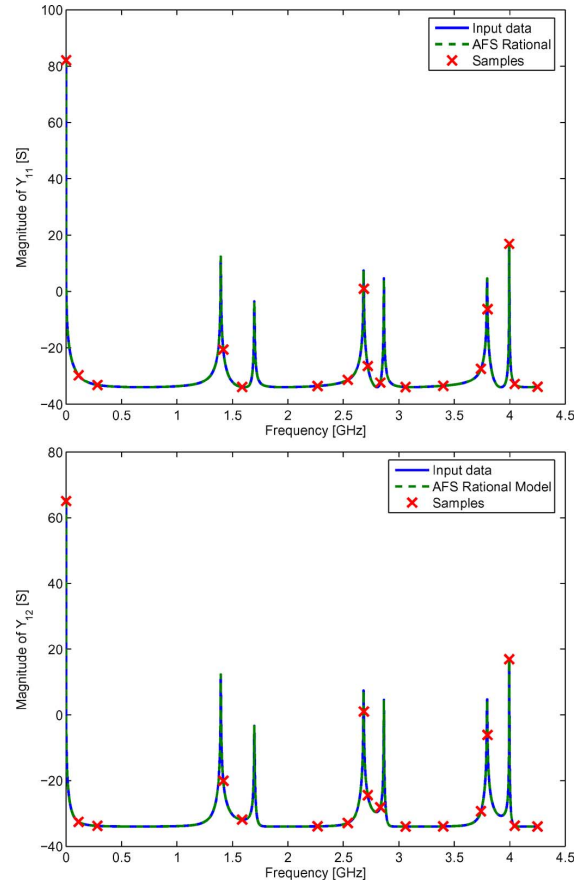The passivity of the macromodel has been checked by computing the eigenvalues of the Hamiltonian matrix M [64] of the minimum state-space system realization, corresponding to the pole-residue representation. It is found that the matrix M has no imaginary eigenvalue; hence, the macromodel is passive [also demonstrated numerically in Fig. 5 by plotting the spectrum of the eigenvalues of $\mathrm{Real}(\boldsymbol{Y}(j\omega))$].

The transmission line is excited by a voltage pulse with 80-ps rise time and 2-ns width.

The port voltages have been computed by using both a full-wave TD solver and the reduced-order model. Fig. 6 shows the
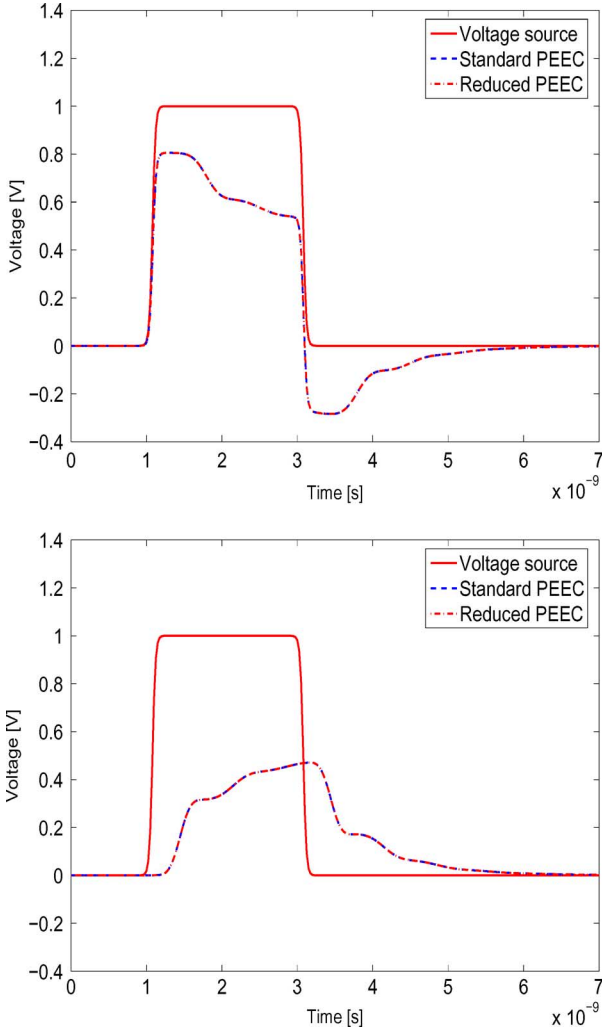
Fig. 6. Port voltages.

Fig. 7. Coplanar microstrips.

Fig. 8. Driclad substrate characteristics. (Top) Magnitude of permittivity (Bottom) Loss tangent.

comparison of the port voltages obtained by the standard PEEC TD solver and the reduced one.

B. Coplanar Microstrip Over a Lossy and Dispersive Substrate

As second test, a coplanar microstrip transmission line on a dispersive and lossy dielectric has been considered. Its geometry is shown in Fig. 7. The conductors are terminated on 50-Ω resistances, and one of them is driven by a 2-V voltage pulse source with 1-ns risetime/falltime and 5-ns width. The time step is 10 ps. The dielectric substrate is constituted by driclad. It exhibits a dispersive and lossy behavior in the range of tens of gigahertz, as confirmed by Fig. 8 showing its permittivity and loss tangent $\tan\delta$, as obtained by using the method described in [65]. The incorporation of the lossy and dispersive dielectric has been accomplished by using the model described in [66]. The global PEEC model is characterized by 720 volume cells, 596 surface cells; the equivalent circuit is constituted by 720 resistances, 518 400 inductances, 355 216 coefficients of potential.

The AFS algorithm selected 14 samples to generate a macromodel of order 20, to ensure a model accuracy of about -45 dB
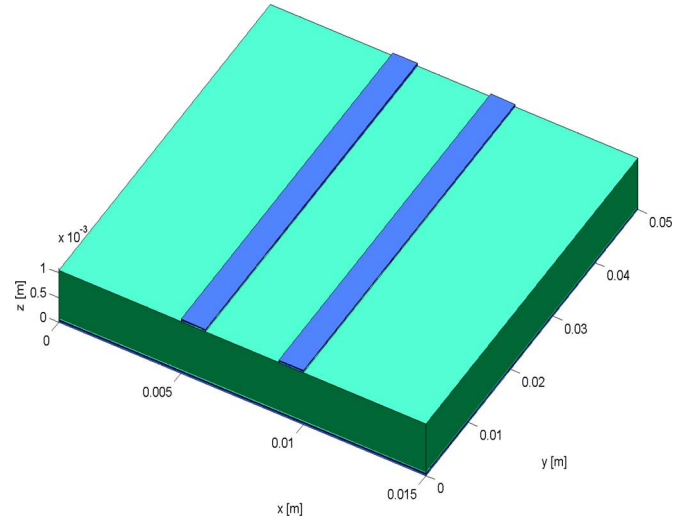
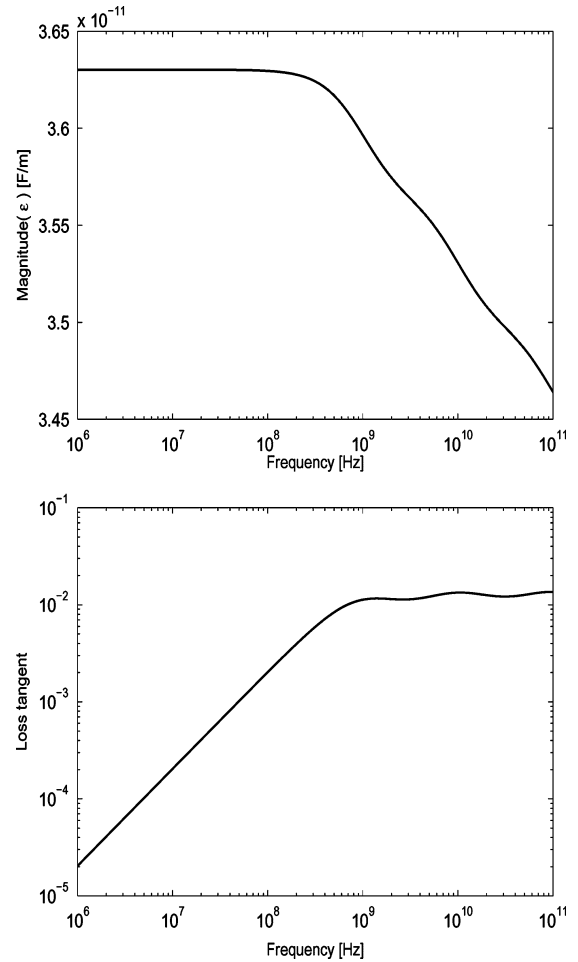over the entire frequency range, as shown in Fig. 9. Table II shows the RMS error convergence as additional frequency samples are added. One of the lines has been driven by a pseudorandom bit sequence with a 250-Mb/s bit rate and a 1-ns risetime; the input and output as well as the near-end and far-end port
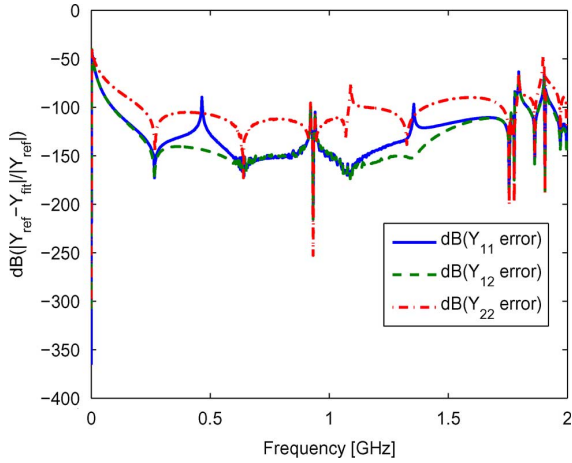
Fig. 9.   AFS relative error of admittances Y_{11}, Y_{12}, Y_{22}.

TABLE II
RMS ERROR (SECTION IV-C)

Frequency samples	RMS error	Frequency samples	RMS error
5	0.578233	10	0.368207
6	0.344633	11	0.352463
7	0.386429	12	0.304229
8	0.380128	13	0.146852
9	0.416428	14	0.000231

voltages have been computed by three methods, explained in Fig. 10, both in the FD and TD.

Figs. 10 show the output voltages of the driven and victim lines; as clearly seen, the macromodel, generated using the AFS, matches very well the results obtained by using the other methods.

Fig. 11 shows the deviation in time of the far-end voltage as computed by using the proposed full-wave AFS-PEEC solver and a standard TD PEEC solver. The maximum deviation remains below 10^{-5} V for late time as well.

Table III summarizes the overall time performance of the full-wave PEEC solvers, namely the TD solver , the FD solver, and the AFS solver. In the same table, the cpu-time ratio, referred to the cpu-time requirement by the AFS-based PEEC solver, is shown.

The AFS-based PEEC solver is faster than the standard TD and FD PEEC solvers. Its time requirements are significantly less than the FD solver and about half of that of the TD solver. Obviously, acceleration techniques such as the FMM, MLFMM [13], [67], QR decomposition [18] can be used to speed up a single frequency sample computation. The main advantage of the AFS algorithm relies on its capability to detect where frequency samples are needed, and thus, to minimize the global number of frequency samples used to generate a rational macromodel. With respect to the TD PEEC solver, the AFS-based PEEC solver allows an easier modeling of frequency-dependent phenomena such as dielectric losses and skin effect, through the use of frequency-dependent basis functions as described in [68].

It is also to be noted that, when broadband modeling is required, the improvements presented in [69] and [70] are needed to preserve accuracy and stability of PEEC models. As the proposed enhanced models are based on a broadband character-
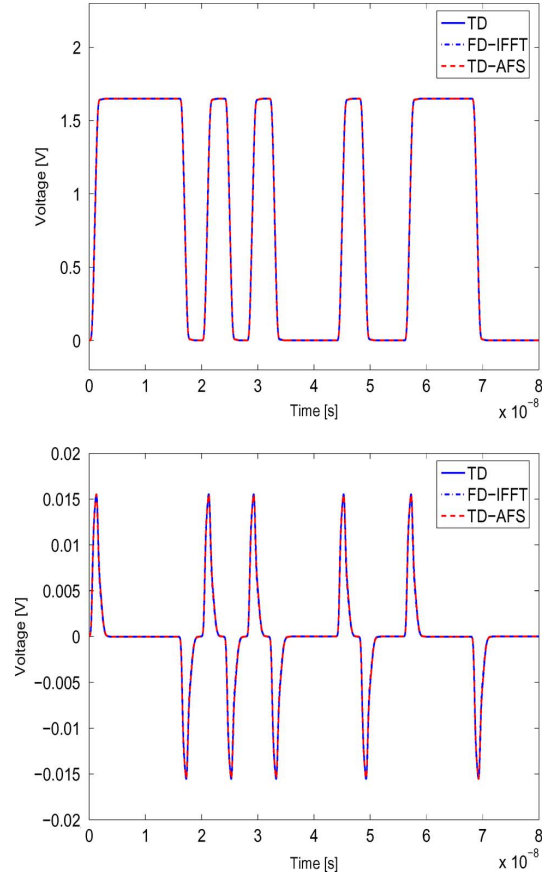

Fig. 10.   Output port voltages. TD refers to the time-domain PEEC solver. FD-IFFT refers to frequency-domain PEEC solver. TD-AFS refers to the time-domain AFS-PEEC solver. (Top) Driven line. (Bottom) Victim line.
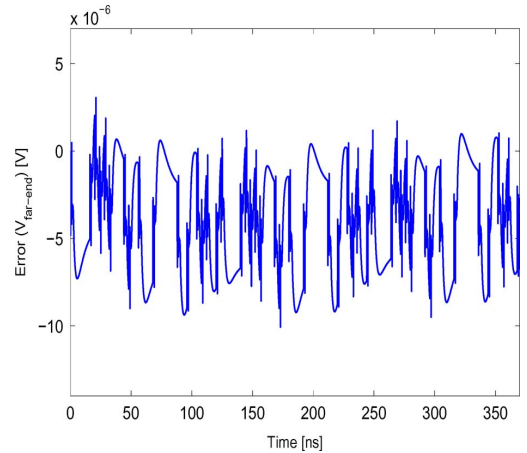

Fig. 11.   Deviation in time of the far-end voltage as computed by using the proposed full-wave AFS-PEEC solver and a standard TD PEEC solver.

ization of the system, the AFS algorithm will be extremely important to speed up the generation of PEEC models. All these issues will be investigated in forthcoming reports.

C. Power Bus

The third application of the new technique is the analysis of the power bus in Fig. 12. It consists of two metallic planes

TABLE III
COMPARISON OF CPU-TIME REQUIREMENTS
FOR THE FULL-WAVE PEEC SOLVERS

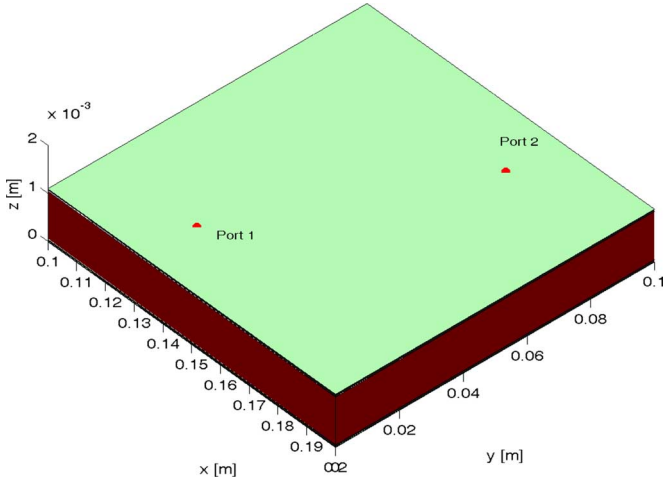| Solver	cpu-time [s]	cpu-time ratio
TD	325	2.16
FD	6670	44.5
AFS	150	1

Fig. 12.   Power bus and port location.

TABLE IV
RMS ERROR (SECTION IV-C)

Frequency samples	RMS error	Frequency samples	RMS error
4	7.527864	12	0.002026
5	5.493942	13	0.050645
6	4.596089	14	0.050632
7	11.216839	15	0.055011
8	1.706640	16	0.000037
9	3.533535	17	0.052350
10	2.962537	18	0.000131
11	0.144425	19	0.000022

separated by a dielectric. The thickness of the planes and dielectric are 50 μm and 1 mm, respectively. The dielectric is modeled to be lossy and dispersive $\varepsilon(s)$. Its complex permittivity has been modeled by using a fourth-order rational model [71] with the distribution of the poles as proposed in [65]. The discretization process has generated 1296 volume cells and 864 surface cells. The overall PEEC circuit consists of 1296 resistances, 1 679 616 inductances, and 746 496 coefficients of potential. Two ports have been considered, located as depicted in Fig. 12. The AFS algorithm has selected an order $n = 27$, using only 19 frequency samples. Table IV shows the RMS error as the AFS algorithm adds additional frequency samples. It can be seen that the RMS error temporarily increases when new resonances are detected, but, once the discovered resonance is modeled, the error decreases again.

Fig. 13 shows the admittances Y_{11} and Y_{12} evaluated using the full PEEC simulation and the AFS-based PEEC solver; in the same figure, the 19 samples used to generate the macromodel are also shown. As can be seen, the agreement is good.

Then, the rational model has been converted into a state-space model. The voltage at the output port, caused by an injected current impulse at the input port, has been calculated. The injected current has a 1-ns risetime/falltime, 5-ns width, and 4 mA of
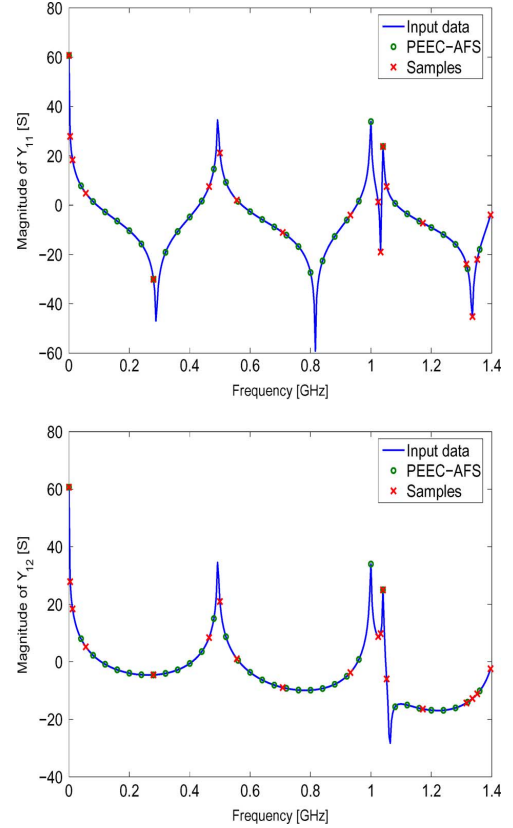

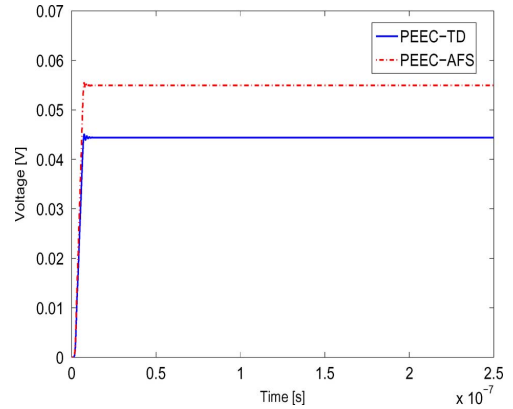Fig. 13.   Power bus admittances Y_{11} and Y_{12}.

Fig. 14.   Output port voltages with (-) and without (--) the dispersive effects of the dielectric.

peak value. Fig. 14 shows a comparison of the voltages as evaluated by an TD PEEC solver, which uses a quasi-static modeling approach of the dielectrics (TD-PEEC), and by the AFS-based PEEC solver (AFS-PEEC), incorporating the dispersive effects of the dielectric. The dispersive effect caused by the smaller values of the dielectric permittivity at higher frequencies (which results into a larger phase velocity at the same frequencies [72]) is evident.

V. CONCLUSION

In this paper, we presented a robust method to generate reduced macromodels based on FD data samples obtained by

means of the PEEC technique. The AFS technique is used to adaptively select the optimal complexity of the model and the location of new frequency samples. The main advantage of the proposed approach is that it avoids convolution integrals when modeling and simulating frequency-dependent phenomena. Furthermore, the AFS technique minimizes the number of required data samples while ensuring a predefined accuracy level. The macromodel can easily be linked to SPICE-like solvers. The proposed algorithm has been used to identify the macromodels of transmission-line-type structures and interconnects, and has been found to be as accurate but much faster than a standard PEEC frequency solver.

REFERENCES

[1] R. F. Harrington, *Field Computation by Moment Methods*. New York: Macmillan, 1968.

[2] A. E. Ruehli and P. A. Brennan, "Efficient capacitance calculations for three-dimensional multiconductor systems," *IEEE Trans. Microw. Theory Tech.*, vol. 21, no. 2, pp. 76–82, Feb. 1973.

[3] J. M. Jin, *The Finite Element Method in Electromagnetics*, 2nd ed. New York: Wiley, 2002.

[4] A. Dounavis, E. Gad, R. Achar, and M. S. Nakhla, "Passive model reduction of multiport distributed interconnects," *IEEE Trans. Microw. Theory Tech.*, vol. 48, no. 12, pp. 2325–2334, Dec. 2000.

[5] R. Achar, P. K. Gunupudi, M. Nakhla, and E. Chiprout, "Passive interconnect reduction algorithm for distributed/measured networks," *IEEE Trans. Circuits Syst., II*, vol. 47, no. 4, pp. 287–301, Apr. 2000.

[6] R. Achar and M. Nakhla, "Simulation of high-speed interconnects," *Proc. IEEE*, vol. 89, no. 5, pp. 693–728, May 2001.

[7] A. E. Ruehli and A. C. Cangellaris, "Progress in the methodologies for the electrical modeling of interconnect and electronic packages," *Proc. IEEE*, vol. 89, no. 5, pp. 740–771, May 2001.

[8] J. Morsey and A. C. Cangellaris, "PRIME: Passive reduction of interconnect models from measured data," in *Proc. Elect. Perform. Electron. Packag.*, Cambridge, MA, 2001, pp. 47–50.

[9] R. Coifman, V. Rokhlin, and S. Wandzura, "The fast multipole method: A pedestrian description," *IEEE Antenna Propag. Mag.*, vol. 35, no. 3, pp. 7–12, Jun. 1993.

[10] L. Greengard, *The Rapid Evaluation of Potential Fields in Particle Systems*. Cambridge, MA: MIT Press, 1988.

[11] W. C. Chew, J.-M. Jin, E. Michielssen, and J. Song, *Fast and Efficient Algorithms in Computational Electromagnetics*, A. House, Ed., Norwood, MA, 2001.

[12] J. M. Song and W. C. Chew, "Multilevel fast-multipole algorithm for solving combined field integral equations of electromagnetic scattering," *Microw. Opt. Technol. Lett.*, vol. 10, no. 1, pp. 15–19, Sep. 1995.

[13] J. M. Song, L. Cai-Cheng, and W. C. Chew, "Multilevel fast-multipole algorithm for solving large-scale problems," *IEEE Trans. Antennas Propag.*, vol. 45, no. 10, pp. 1488–1493, Oct. 1997.

[14] K. Sertel and J. L. Volakis, "Multilevel fast multipole method solution of volume integral equations using parametric geometry modeling," *IEEE Trans. Antennas Propag.*, vol. 52, no. 7, pp. 1686–1692, Jul. 2004.

[15] E. Bleszynski, M. Bleszynski, and T. Jaroszewicz, "AIM: Adaptive integral method for solving large-scale scattering and radiation problems," *Numer. Alg.*, vol. 31, no. 5, pp. 1225–1251, 1996.

[16] J. R. Phillips and J. K. White, "A precorrected-FFT method for electrostatic analysis of complicated 3-D structures," *IEEE Trans. Comput.-Aided Design Integr. Circuits Syst.*, vol. 16, no. 10, pp. 1059–1072, Oct. 1997.

[17] D. Gope and V. Jandhyala, "Oct-tree-based multilevel low-rank decomposition algorithm for rapid 3-D parasitic extraction," *IEEE Trans. Comput.-Aided Design*, vol. 23, no. 11, pp. 1575–1580, Nov. 2004.

[18] D. Gope, A. E. Ruehli, and V. Jandhyala, "Speeding up PEEC partial inductance computation using a QR-based algorithm," *IEEE Trans. Very Large Scale Integr. (VLSI) Syst.*, vol. 15, no. 1, pp. 60–68, Jan. 2007.

[19] L. T. Pillage and R. A. Rohrer, "Asymptotic waveform evaluation for timing analysis," *IEEE Trans. Comput.-Aided Design*, vol. 9, no. 4, pp. 352–366, Apr. 1990.

[20] K. Gallivan, E. Grimme, and P. Van Dooren, "Asymptotic waveform evaluation via a Lanczos method," *Appl. Math.*, vol. 7, no. 5, pp. 75–80, Sep. 1994.

[21] E. Chiprout and M.S. Nakhla, *Asymptotic Waveform Evaluation*. Norwell, MA: Kluwer, 1994.

[22] R. W. Freund and P. Feldmann, "Efficient small-signal circuit analysis and sensitivity computatations with the PVL algorithm," presented at the Int. Conf. Comput.-Aided Design, San Jose, CA, Nov. 1994.

[23] R. W. Freund and P. Feldmann, "Efficient linear circuits analysis by Padé approximation via Lanczos process," *IEEE Trans. Comput.-Aided Design*, vol. 14, no. 5, pp. 639–649, May 1995.

[24] K. Gallivan, E. Grimme, and P. Van Dooren, "A rational Lanczos algorithm for model reduction," *Numer. Alg.*, vol. 12, pp. 33–63, 1996.

[25] N. Marques, M. Kamon, J. White, and L. M. Silveira, "A mixed nodal-mesh formulation for efficient extraction and passive reduced-order modeling of 3D interconnects," presented at the Design Autom. Conf., San Francisco, CA, Jun. 1998, 35.

[26] Z. Bai, R. D. Slone, W. T. Smith, and Q. Ye, "Error bound for reduced system model by Padé approximation via the Lanczos process," *IEEE Trans. Comput.-Aided Design*, vol. 18, no. 2, pp. 133–141, Feb. 1999.

[27] A. Odabasioglu, M. Celik, and L. T. Pileggi, "PRIMA: Passive reduced-order interconnect macromodeling algorithm," *IEEE Trans. Comput.-Aided Design*, vol. 17, no. 8, pp. 645–654, Aug. 1998.

[28] A. E. Ruehli, "Equivalent circuit models for three dimensional multiconductor systems," *IEEE Trans. Microw. Theory Tech.*, vol. MTT-22, no. 3, pp. 216–221, Mar. 1974.

[29] W. Pinello, A. C. Cangellaris, and A. E. Ruehli, "Hybrid electromagnetic modeling of noise interactions in packaged electronics based on the partial-element equivalent circuit formulation," *IEEE Trans. Microw. Theory Tech.*, vol. MTT-45, no. 10, pp. 1889–1896, Oct. 1997.

[30] J. Cullum, A. Ruehli, and T. Zhang, "A method for reduced-order modeling and simulation of large interconnect circuits and its application to PEEC models with retardation," *IEEE Trans. Circuits Syst., II*, vol. 47, no. 4, pp. 261–373, Apr. 2000.

[31] G. Burke, E. Miller, S. Chakrabarti, and K. Demarest, "Using model-based parameter estimation to increase the efficiency of computing electromagnetic transfer functions," *IEEE Trans. Magn.*, vol. 25, no. 4, pp. 2807–2809, Jul. 1989.

[32] E. K. Miller, "Model-based parameter estimation in electromagnetics. I. Background and theoretical development," *IEEE Antenna Propag. Mag.*, vol. 40, no. 1, pp. 42–52, Feb. 1998.

[33] E. K. Miller, "Model-based parameter estimation in electromagnetics. II. Applications to EM observables," *IEEE Antenna Propag. Mag.*, vol. 40, no. 2, pp. 51–65, Apr. 1998.

[34] E. K. Miller, "Model-based parameter estimation in electromagnetics. III. Applications to EM integral equations," *IEEE Antenna Propag. Mag.*, vol. 40, no. 3, pp. 49–66, Jun. 1998.

[35] B. Gustavsen and A. Semlyen, "Rational approximation of frequency domain responses by vector fitting," *IEEE Trans. Power App. Syst.*, vol. 14, no. 3, pp. 1052–1061, Jul. 1999.

[36] B. Gustavsen, "Frequency-dependent modeling of power transformers with ungrounded windings," *IEEE Trans. Power App. Syst.*, vol. 19, no. 3, pp. 1328–1334, Jul. 2004.

[37] S. Grivet-Talocia, H.-M. Huang, A. E. Ruehli, F. Canavero, and I. M. (Abe) Elfadel, "Transient analysis of lossy transmission lines: An efficient approach based on the method of characteristics," *IEEE Trans. Adv. Packag.*, vol. 27, no. 1, pp. 45–56, Feb. 2004.

[38] M. S. Sarto, "A new model for the FDTD analysis of the shielding performances of thin composite structures," *IEEE Trans. Electromagn. Compat.*, vol. 41, no. 4, pp. 298–306, Nov. 1999.

[39] G. Antonini, A. Ciccomancini Scogna, and A. Orlandi, "Time domain modelling of PCB discontinuities," in *Electrical Engineering and Electromagnetics*, C. A. Brebbia and D. Polyak, Eds. Billerica, MA: WIT Press, 2003, pp. 109–118.

[40] J. Brittingham, E. Miller, and J. Willows, "Pole extraction from real-frequency information," *Proc. IEEE*, vol. 68, no. 2, pp. 263–273, Feb. 1980.

[41] T. Dhaene, J. Ureel, N. Faché, and D. De Zutter, "Adaptive frequency sampling algorithm for fast and accurate S-parameter modeling of general planar structures," in *Proc. IEEE Int. Microw. Symp. 1995, MTT-S*, Orlando, FL, pp. 1427–1430.

[42] A. W. Glisson and D. R. Wilson, "Simple and efficient numerical methods for problems of electromagnetic radiation and scattering from surfaces," *IEEE Trans. Antennas Propag.*, vol. 28, no. 5, pp. 593–603, Sep. 1980.

[43] S. M. Rao, D. R. Wilton, and A. W. Glisson, "Electromagnetic scattering by surfaces of arbitrary shape," *IEEE Trans. Antennas Propag.*, vol. 30, no. 3, pp. 409–418, May 1982.

[44] S. M. Rao and D. R. Wilton, "Transient scattering by conducting surfaces of arbitrary shape," *IEEE Trans. Antennas Propag.*, vol. 39, no. 1, pp. 56–61, Jan. 1991.

[45] B. M. Kolundzija and B. D. Popovic, "Entire-domain Galerkin method for analysis of metallic antennas and scatterers," *Proc. Inst. Elect. Eng. H*, vol. 140, no. 1, pp. 1–10, Jan. 1993.

[46] J. J. H. Wang, *Generalized Moment Method in Electromagnetics*. New York: Wiley, 1991.

[47] A. E. Ruehli, J. Garrett, and C. R. Paul, "Circuit models for 3D structures with incident fields," in *Proc. IEEE Int. Symp. Electromagn. Compat.*, Dallas, TX, Aug.1993, pp. 28–31.

[48] B. Gustavsen, "Computer code for rational approximation of frequency dependent admittance matrix," *IEEE Trans. Power Del.*, vol. 17, no. 4, pp. 97–104, Oct. 2002.

[49] T. Kailath, *Linear Systems*. Englewood Cliffs, NJ: Prentice-Hall, 1980.

[50] C. T. Chen, *Linear System Theory and Design*. New York: Holt, Rinehart, Winston, 1984.

[51] A. Ruberti and S. Monaco, *Teoria dei Sistemi*. Bologna, Italy: Pitagora Editrice, 1998.

[52] R. Neumayer, A. Steltzer, F. Haslinger, and R. Weigel, "On the synthesis of equivalent-circuit models for multiports characterized by frequency-dependent parameters," *IEEE Trans. Microw. Theory Tech.*, vol. 50, no. 12, pp. 2789–2796, Dec. 2002.

[53] C. Ho, A. Ruehli, and P. Brennan, "The modified nodal approach to network analysis," *IEEE Trans. Circuits Syst.*, vol. 22, no. 6, pp. 504–509, Jun. 1975.

[54] *HSPICE,* Avanti Inc., Cambell, CA, 1999.

[55] R. Achar and M. Nakhla, "Simulation of high-speed interconnects," *Proc. IEEE*, vol. 89, no. 5, pp. 693–728, May 2001.

[56] T. Mangold and P. Russer, "Full-wave modeling and automatic equivalent circuit generation of millimeter-wave planar and multilayer structures," *IEEE Trans. Microw. Theory Tech.*, vol. 47, no. 6, pp. 851–858, Jun. 1999.

[57] G. Antonini, "Spice compatible equivalent circuits of rational approximation of frequency domain responses," *IEEE Trans. Electromagn. Compat.*, vol. 45, no. 3, pp. 502–512, Aug. 2003.

[58] G. Antonini, Deschrijver and T. Dhaene, "Adaptive building of accurate and stable PEEC models for EMC applications," in *Proc. EMC Eur. 2006 Symp.*, Barcelona, Spain, Sep., pp. 51–56.

[59] T. Dhaene, "Automated fitting and rational modeling algorithm for EM-based S-parameter data," in *Proc. 6th Int. Conf. Appl. Parallel Comput. (PARA 2002),* (V. L. Springer Lecture Notes in Computer Science Edition), Espoo, Finland, May, pp. 99–105.

[60] D. Deschrijver and T. Dhaene, "Efficient GA-inspired macro-modeling of general LTI multi-port systems," in *Proc. 8th IEEE Workshop Signal Propag. Interconnects, SPI 2004*, Heidelberg, Germany, pp. 95–98.

[61] S. Grivet-Talocia, "Enforcing passivity by perturbation of Hamiltonian matrix," *IEEE Trans. Circuits Syst.*, vol. 51, no. 9, pp. 1755–1769, Feb. 2004.

[62] U. Beyer and F. Smieja, "Data exploration with reflective adaptive models," *Computational Statistics and Data Analysis*, vol. 22, no. 2, pp. 193–211, 1996.

[63] B. Gustavsen, "Improving the pole relocating properties of vector fitting," *IEEE Trans. Power Del.*, vol. 21, no. 3, pp. 1587–1592, Jul. 2006.

[64] S. Boyd, L. El Ghaoui, E. Feron, and V. Balakrishnan, *Linear Matrix Inequalities in System and Control Theory*. Philadelphia, PA: SIAM, 1994.

[65] A. E. Engin, W. Mathis, W. John, G. Sommer, and H. Reichl, "Time domain modeling of lossy substrates with constant loss tangent," in *Proc. 6th IEEE Workshop Signal Propag. Interconnects*, Heidelberg, Germany, May 2004, pp. 151–154.

[66] G. Antonini, A. E. Ruehli, and A. Haridass, "Including dispersive dielectrics in PEEC models," in *Proc. Elect. Perform. Electron. Packag.*, Princeton, NJ, Oct. 2003, pp. 349–352.

[67] W. C. Chew, J.-M. Jin, C.-C. Lu, E. Michielssen, and J. M. Song, "Fast solution methods in electromagnetics," *IEEE Trans. Antennas Propag.*, vol. 45, no. 3, pp. 533–543, Mar. 1997.

[68] G. Antonini and A. E. Ruehli, "Combined loss mechanism and stability model for the partial element equivalent circuit technique," presented at the Appl. Comput. Electromagn. Conf., Verona, Italy, Mar. 2007.

[69] G. Antonini, "Broadband PEEC models for ultra wide band applications," in *Proc. EMC Eur. Workshop 2005: EMC Wireless Syst.*, Rome, Italy, Sep., pp. 271–274.

[70] G. Antonini, D. Deschrijver, and T. Dhaene, "Broadband macromodels for retarded partial element equivalent circuit (rPEEC) method," *IEEE Trans. Electromagn. Compat.*, vol. 49, no. 1, pp. 34–48, Feb. 2007.

[71] G. Antonini, A. E. Ruehli, and A. Haridass, "PEEC equivalent circuits for dispersive dielectrics," in *Proc. Piers—Progress Electromagn. Res. Symp.*, Pisa, Italy, Mar. 2004, pp. 767–770.

[72] J. D. Jackson, *Classical Electrodynamics*. New York: Wiley, 1962.

Giulio Antonini (M'94–SM'05) received the Laurea degree (*summa cum laude*) in electrical engineering from the University of L'Aquila, L'Aquila, Italy, in 1994, and the Ph.D. degree in electrical engineering from the University of Rome "La Sapienza," Rome, Italy, in 1998.

Since 1998, he has been with the UAq Electromagnetic Compatibility (EMC) Laboratory, Department of Electrical Engineering, University of L'Aquila, where he is currently an Associate Professor. His current research interests include EMC analysis, numerical modeling, and the field of signal integrity for high-speed digital systems. He is the author or coauthor of more than 120 technical papers, three book chapters, and has given nine keynote lectures. He is the holder of one European Patent. Since 1998, he has been collaborating with the IBM T. J. Watson Research Center, where he is engaged in the development of algorithms for partial element equivalent circuit (PEEC) modeling.

Dr. Antonini is the recipient of the IEEE TRANSACTIONS ON ELECTROMAGNETIC COMPATIBILITY Best Paper Award in 1997, the Computer Simulation Technology (CST) University Publication Award in 2004, the IBM Shared University Research Award in 2004, 2005, and 2006, and the Technical Achievement Award from the IEEE EMC Society "for innovative contributions to computational electromagnetic on the PEEC technique for EMC applications" in 2006. He is the Vice Chairman of the dell'IEEE EMC Italy Chapter, a member of the TC-9 committee of the IEEE EMC Society, and the Vice Chairman of the TC-10 Committee of the same IEEE Society. He is on the technical program committees of the Date Conference and serves as a reviewer in a number of IEEE journals. He has chaired several special sessions at international conferences.

Dirk Deschrijver was born in Tielt, Belgium, on September 26, 1981. He received the Master's degree (*licentiaat*) in computer science, and the Ph.D. degree from the University of Antwerp, Antwerp, Belgium, in 2003 and 2007, respectively.

From May to October 2005, he was a Marie Curie Fellow in the Scientific Computing Group, Eindhoven University of Technology, Eindhoven, The Netherlands. He is currently a Postdoctoral Fellow in the Department of Information Technology, Ghent University, Ghent, Belgium. His current research interests include rational least-squares approximation, orthonormal rational functions, system identification, and broadband macromodeling techniques.

Tom Dhaene (M'94–SM'05) was born in Deinze, Belgium, on June 25, 1966. He received the Ph.D. degree in electrotechnical engineering from the University of Ghent, Ghent, Belgium, in 1993.

From 1989 to 1993, he was a Research Assistant in the Department of Information Technology, University of Ghent, where he is engaged in research on different aspects of full-wave electromagnetic (EM) circuit modeling, transient simulation, and time-domain characterization of high-frequency and high-speed interconnections. In 1993, he joined the Electronic Design Automation (EDA) company Alphabit (now part of Agilent). He was one of the key developers of the planar EM simulator ADS Momentum, and he is the principal developer of the multivariate EM-based adaptive metamodeling tool ADS Model Composer. Since September 2000, he has been a Professor in the Department of Mathematics and Computer Science, University of Antwerp, Antwerp, Belgium. Since October 2007, he is a Full Professor in the Department of Information Technology (INTEC), Ghent University. His modeling and simulation EDA software is successfully used by academic, government, and business organizations worldwide for the study and design of high-speed electronics and broadband communication systems. He is the author or coauthor of more than 100 peer-reviewed papers and abstracts in international conference proceedings, journals, and books. He is the holder of two U.S. patents.